

# ArtCrafter: Text-Image Aligning Style Transfer via Embedding Reframing

Nisha Huang<sup>1,2</sup>, Kaer Huang<sup>3</sup>, Yifan Pu<sup>1</sup>, Jiangshan Wang<sup>1</sup>, Jie Guo<sup>2</sup>,  
Yiqiang Yan<sup>3</sup>, Xiu Li<sup>1\*</sup>

<sup>1</sup>Tsinghua University <sup>2</sup>Peng Cheng Laboratory <sup>3</sup>Lenovo Research

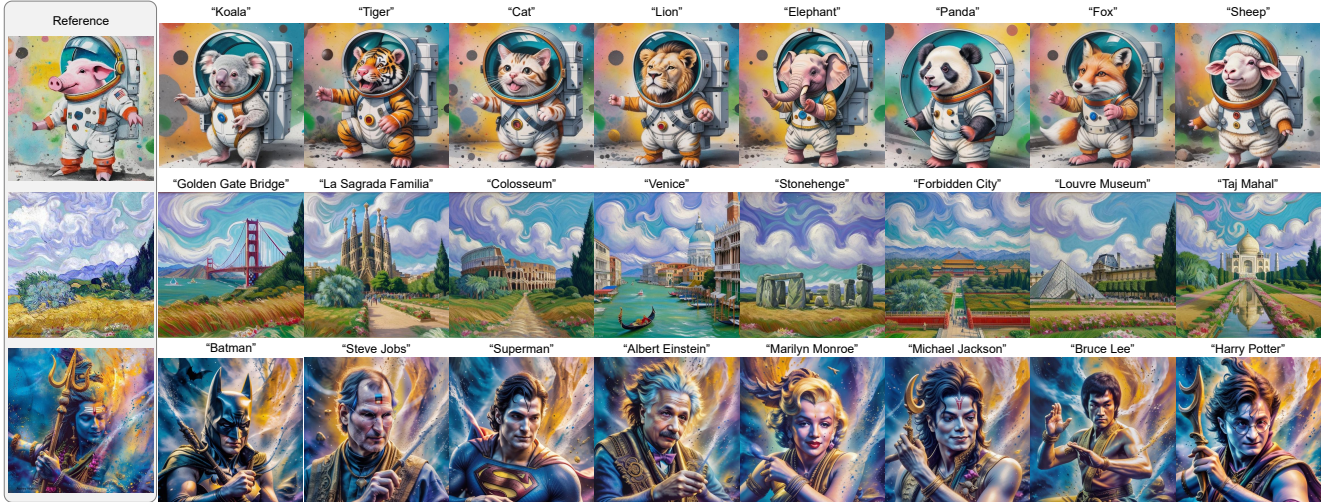


Figure 1. **ArtCrafter generation results.** By injecting the features of the reference images and text prompts during the diffusion process, our method is capable of capturing and generating a faithful style representation.

## Abstract

Recent years have witnessed significant advancements in text-guided style transfer, primarily attributed to innovations in diffusion models. These models excel in conditional guidance, utilizing text or images to direct the sampling process. However, despite their capabilities, direct conditional guidance approaches often face challenges in balancing the expressiveness of textual semantics with the diversity of output results while capturing stylistic features. To address these challenges, we introduce ArtCrafter, a novel framework for text-to-image style transfer. Specifically, we introduce an attention-based style extraction module, meticulously engineered to capture the subtle stylistic elements within an image. This module features a multi-layer architecture that leverages the capabilities of perceiver attention mechanisms to integrate fine-grained information. Additionally, we present a novel text-image aligning augmentation component that adeptly balances control over both modalities, enabling the model to efficiently map image and text embeddings into a shared feature space. We achieve

*this through attention operations that enable smooth information flow between modalities. Lastly, we incorporate an explicit modulation that seamlessly blends multimodal enhanced embeddings with original embeddings through an embedding reframing design, empowering the model to generate diverse outputs. Extensive experiments demonstrate that ArtCrafter yields impressive results in visual stylization, exhibiting exceptional levels of stylistic intensity, controllability, and diversity.*

## 1. Introduction

Diffusion-based text-to-image generations [29, 33] have achieved notable progress in the realms of personalization and customization, especially in consistent synthesis such as identity protection [23, 44], object customization [15, 27] and style transfer [5, 6, 8, 16, 20, 52, 53]. In particular, text-guided style transfer focuses on fine-grained style representation that encompasses abstract concepts like texture, color, composition, and material, to create a spectrum of personalized outputs grounded in the textual semantic essence.

\*Corresponding authors.

Current methods often use pre-trained diffusion models [10, 11, 17, 24, 25, 35, 42, 43, 48] for stylization tasks, enhancing model features by adding a trainable adapter module without full retraining. In text-to-image style transfer applications, adapter-based methods shape the style and content of the output by adjusting the condition guidance scales over the input image and text prompts. However, we have identified three main issues with previous research: **1)** Inadequate artistic style representation. For convenience, traditional image encoder architectures and training data primarily focus on natural images, which limits their ability to capture the intricate textures and stylistic nuances of artistic images. **2)** The text-guided conditions underperform expectations. As shown in Fig. 2, the usual adapter-based [48] method fails to deliver the expected results when the text condition “*Fashion shoes*” is used. This discrepancy arises because the amount of information in image and text embeddings are not equivalent, yet adapter-based methods [10, 11, 24, 25, 35, 42, 48] often directly concatenate the two without addressing the imbalance and disparity, leading to image data overshadowing text prompts during the sampling process. **3)** Lack of output diversity. The constrained liberation of textual guidance results in generated outputs that closely resemble the reference images, thereby limiting the diversity of the results.

To tackle the aforementioned issues, we introduce ArtCrafter, a crafted embedding reframing solution based on diffusion models, designed specifically for text-guided stylization tasks. The proposed ArtCrafter consists of three components: **1)** Attention-based style extraction (Sec. 3.2) leverages multi-level features to capture complicated stylistic information, ensuring more coherent and accurate stylistic encoding. It employs perceiver attention and a multi-layer architecture to capture both local and global stylistic elements. Additionally, we introduce the ArtMarket dataset, which pairs art images with text descriptions, allowing us to fine-tune an encoder initially trained on natural images. This approach retains strong generalization capabilities while being sensitive to the unique visual elements of artistic styles. **2)** The text-image aligning augmentation (Sec. 3.3) module improves the alignment of image and text embeddings through crafted attentional interactions, mapping them into a shared feature space. This alignment ensures that the generated images reflect both the style of the reference image and the content of the textual conditions, thus enhancing controllability. **3)** The explicit modulation component (Sec. 3.4) enhances the adaptability of conventional fusion techniques through the implementation of linear interpolation and concatenation schemes. This method facilitates the merging of original image and text embeddings with multimodal embeddings, yielding enhanced embeddings. It allows ArtCrafter to generate images that are relevant to the text prompts and exhibit diverse visual rep-



Figure 2. **Generic adapter-based vs. ArtCrafter generation results.** Given a content description of “*Fashion Shoes*”, generic adapter-based generation (above) results in unaligned results and limited result diversity. In contrast, our approach (below) generates text-aligned content as well as multiple shoe types.

resentations. Our main contributions can be summarized as follows:

- We present ArtCrafter, a lightweight adapter designed to enhance the capabilities of pre-trained diffusion models in the domain of text-guided stylized image generation. Our approach centers on attention-based style feature extraction, adeptly capturing both local and global features.
- We propose an innovative text-image aligning augmentation module that facilitates robust interaction between reference images and textual descriptions within a shared feature space, significantly amplifying the impact of text prompts on the generative process.
- The explicit modulation within ArtCrafter boosts the multimodal embeddings utilization while surpassing conventional methods in flexibility and diversity. Furthermore, ArtCrafter is compatible with additional control conditions and outperforms the state-of-the-art approaches across various experimental benchmarks.

## 2. Related Work

**Attention Control in diffusion models.** Following the remarkable progress made in the field of pre-training text-to-image diffusion models [14, 29, 33, 38], a series of image editing efforts [1, 2, 46, 50] have emerged. Hertz *et al.* [12] propose the Prompt-to-Prompt method, which achieves text-based partial image editing and generates edited images that conform to textual conditions by replacing original vocabulary and cross-attention maps. Plug-and-play [49] utilizes the spatial features and self-attention mapping of the original image to guide the diffusion model for text-guided image-to-image translation while preserving the spatial layout of the original image. Later, MasaCtrl [4] proposes a mutual self-attention control technique for coherent image editing. Consistent image editing is achieved by preserving the key and value of the self-attention layer of the source image while conditioning the model with desired text prompts. Recently, StyleID [6] proposes a style migration method without training by injecting styles in the self-attention layer and introduces query preservation, attention

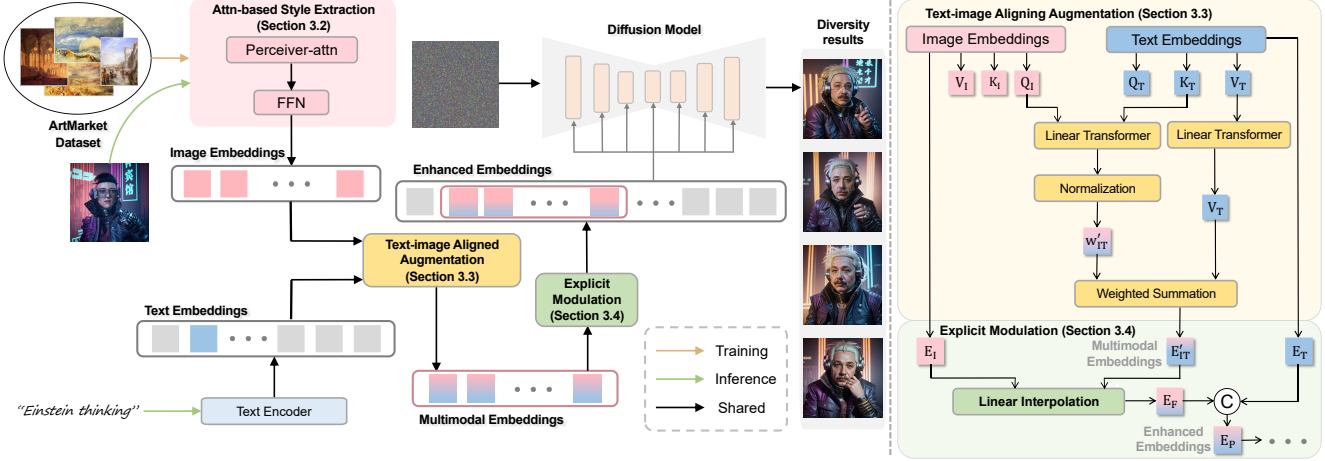


Figure 3. **Our proposed ArtCrafter’s overview pipeline consists of three modules:** 1) Attention-based style extraction captures fine-grained style features from images using multi-head perceiver attention and feed-forward networks. 2) Text-image aligning augmentation transfers the style embedding to the textual space to improve the image-text consistency in the generated images. 3) Explicit modulation seamlessly combines multimodal embeddings with original image embeddings and text embeddings in different ways, increasing the versatility and diversity of the method.

temperature scaling, and initial latent AdaIN techniques to minimize the impact of style injection on the original content.  $Z^*$  [8] shows how to extract style information directly from style images and fuse it with content images without training by means of an attentional reweighting strategy. Unlike the methods mentioned above, our approach focuses on the interaction of image and text information, as well as a balance for guiding the generation process.

**Text-guided style transfer.** Stylization [9, 26, 30, 47] is to control the content through text and make the generated image consistent while keeping the style of the reference image. StyleDrop [39] is a method of achieving arbitrary style synthesis from a small number of stylized images and textual descriptions by efficiently fine-tuning a small number of parameters of a pre-trained model and combining iterative training with feedback to improve the quality of the generated images. The well-received work IP-Adapter [48] improves stylization image generation by introducing the embedding of input images in an additional layer of cross-attention, which enhances the model’s ability to capture features from the input images. Building on the IP-Adapter, InstantStyle [42] manually selects specific attention layers to control the style of the output. However, for the IP-Adapter conditioned on natural images, the expected conditioning of the input artistic image does not always work. Visual Style Prompting (VSP) [19] captures stylistic details by fusing key features of the reference image in a later self-attention layer while preserving the content consistency of the original image. However, compared to cross-attention, self-attention provides a weaker ability to control the semantic content of the generated image. Style Aligned [13] attempts to align style and content through a shared attention mechanism. However, it generates results with content

information leaked from the style image, and there are challenges in disentangling content and style. StyleShot [10] is trained by a two-stage style control method. However, detailed information within the control is easily lost due to sparse rows and columns. Furthermore, [10], [25], and [46] only trained on the art-text datasets, making it difficult to broadly adapt to arbitrary stylistic features.

### 3. Method

The overall architecture of ArtCrafter is shown in Fig. 3. As reviewed in Sec. 3.1, ArtCrafter is built upon diffusion model [33, 37]. In Sec. 3.2, we introduce attention-based style extraction, which captures multi-level style information by perceiver attention and multi-layer design. Text-image aligning augmentation (Sec. 3.3) allows the model to dynamically weigh the importance of different parts of the text prompt. This enables a more nuanced and context-aware generation process, resulting in images that are more closely related to the text prompt. Explicit modulation (Sec. 3.4) provides an effective way to combine textual and visual information, enabling the model to generate images that are both relevant to the text prompt and have diverse visual representations.

#### 3.1. Preliminary

Diffusion model [33] consists of two processes: a forward process, which incrementally adds Gaussian noise  $\epsilon$  to the data  $x_0$  through a Markov chain. Additionally, a denoising process generates samples from Gaussian noise  $x_T \sim N(0, 1)$  with a learnable denoising model  $\epsilon_\theta(x_t, t, c)$  parameterized by  $\theta$ . This denoising model  $\epsilon_\theta(\cdot)$  is implemented with U-Net [34] and trained with a mean-squared

loss derived by a simplified variant of the variational bound:

$$\mathcal{L} = \mathbb{E}_{t, x_0, \epsilon} [\|\epsilon - \hat{\epsilon}_\theta(x_t, t, c)\|^2], \quad (1)$$

where  $c$  denotes an optional condition. In the diffusion model,  $c$  is generally represented by the text embeddings  $E_T$  encoded from a text prompt using CLIP [31] and integrated into the diffusion model through the following designed module (Sec. 3.4).

### 3.2. Attention-based Style Extraction

This section elaborates on the style extraction method, which enhances the style encoding capabilities by integrating fine-grained features through a multi-layer architecture. The objective is to capture intricate style details from images by leveraging perceiver attention [18] and position-wise feed-forward network (FFN) [41].

Given the reference image, we obtain the input image embeddings through CLIP, denoted as  $x$ . The latent variables  $z$  are initialized as a tensor with a shape of  $(1, N, D)$ , where  $N$  is the number of queries and  $D$  is the dimension of the latent space, and are normalized by dividing by the square root of  $D$  to stabilize the training process:

$$z = \frac{\mathcal{N}(0, 1)}{D^{0.5}}. \quad (2)$$

To match the batch size of the input  $x$ , we expand the latent variable  $z$  by repeating it along the batch dimension. This process can be represented as:

$$z = z \otimes \mathbf{1}_B, \quad (3)$$

where  $\mathbf{1}_B$  is a tensor of ones with shape  $(B, 1, 1)$ , and  $B$  is the batch size of  $x$ . This operation results in a tensor  $z$  with shape  $(B, N, D)$ , where  $N$  is the number of queries and  $D$  is the dimension of the latent space.

The perceiver attention mechanism denoted as P-Attn, is then applied to update the latent variables by attending to the input  $x$  and the repeated latent variables:

$$\text{P-Attn}(x, z) = \text{softmax}\left(\frac{zx^T}{\sqrt{d_k}}\right) \cdot x, \quad (4)$$

$$z' = \text{P-Attn}(x, z) + z, \quad (5)$$

where  $d_k$  is the dimension of the key tensor, typically equal to  $D$ . This operation allows the model to selectively focus on different parts of the input data based on the learnable latent variables.

The FFN consists of two linear transformations with a GELU activation function in between:

$$\text{FFN}(z') = W_2 \cdot \text{GELU}(W_1 \cdot z' + b_1) + b_2, \quad (6)$$

where  $W_1$  and  $W_2$  are weight matrices, and  $b_1$  and  $b_2$  are bias terms. The output  $E_I$  represents the style embeddings extracted from the input image, obtained by combining the FFN output and the updated latent variables  $z'$ :

$$E_I = \text{FFN}(z') + z'. \quad (7)$$

### 3.3. Text-Image Aligning Augmentation

The text-image aligning augmentation method is designed to dynamically prioritize different aspects of the text prompt by leveraging cross-attention mechanisms. This module allows the model to integrate image and text embeddings more effectively, projecting them into a shared feature space where their interactions can be more nuanced.

We start by transforming the image prompt embeddings  $E_I$  and the text prompt embeddings  $E_T$  into query, key, and value matrices through linear layers. These transformations are represented as:

$$Q_I = W_{Q_I}E_I, \quad K_T = W_{K_T}E_T, \quad V_T = W_{V_T}E_T. \quad (8)$$

$W_{Q_I}$ ,  $W_{K_T}$ , and  $W_{V_T}$  are the weight matrices associated with the query for images, key for text, and value for text, respectively. The attention weights  $\mathbf{w}_{IT}$  are calculated by taking the dot product of the query matrix  $Q_I$  and the key matrix  $K_T$ , scaled by the square root of the key dimension  $d_{k_T}$  to prevent gradient disappearance:

$$\mathbf{w}_{IT} = \frac{Q_I K_T^T}{\sqrt{d_{k_T}}}. \quad (9)$$

The softmax function is then applied to these raw attention scores to obtain the normalized attention weights  $\mathbf{w}'_{IT}$ :

$$\mathbf{w}'_{IT} = \text{softmax}(\mathbf{w}_{IT}). \quad (10)$$

Using the normalized attention weights  $\mathbf{w}_{IT}$ , we compute the weighted sum of the value matrix  $V_T$  to generate the multimodal embeddings  $E'_{IT}$ :

$$E'_{IT} = \mathbf{w}'_{IT} \cdot V_T. \quad (11)$$

$E'_{IT}$  captures the multimodal context more effectively, allowing the model to generate images that are more closely aligned with the semantic content of the text prompt. This approach is particularly beneficial in scenarios where the textual and visual information needs to be tightly integrated to produce coherent outputs.

### 3.4. Explicit Modulation

The explicit modulation solves the problem of lack of flexibility in traditional fusion methods by seamlessly fusing the image embeddings with the text-image aligning augmented multimodal embeddings utilizing linear interpolation. Specifically, we fuse the image embeddings  $E_I$  with the multimodal embeddings  $E'_{IT}$  through linear interpolation:

$$E_F = \alpha E_I + (1 - \alpha) E'_{IT}, \quad (12)$$

where  $\alpha$  is a predefined constant controlling the fusion ratio between the original and enhanced embeddings. Ultimately, we concatenate the fused image embeddings  $E_F$  with the

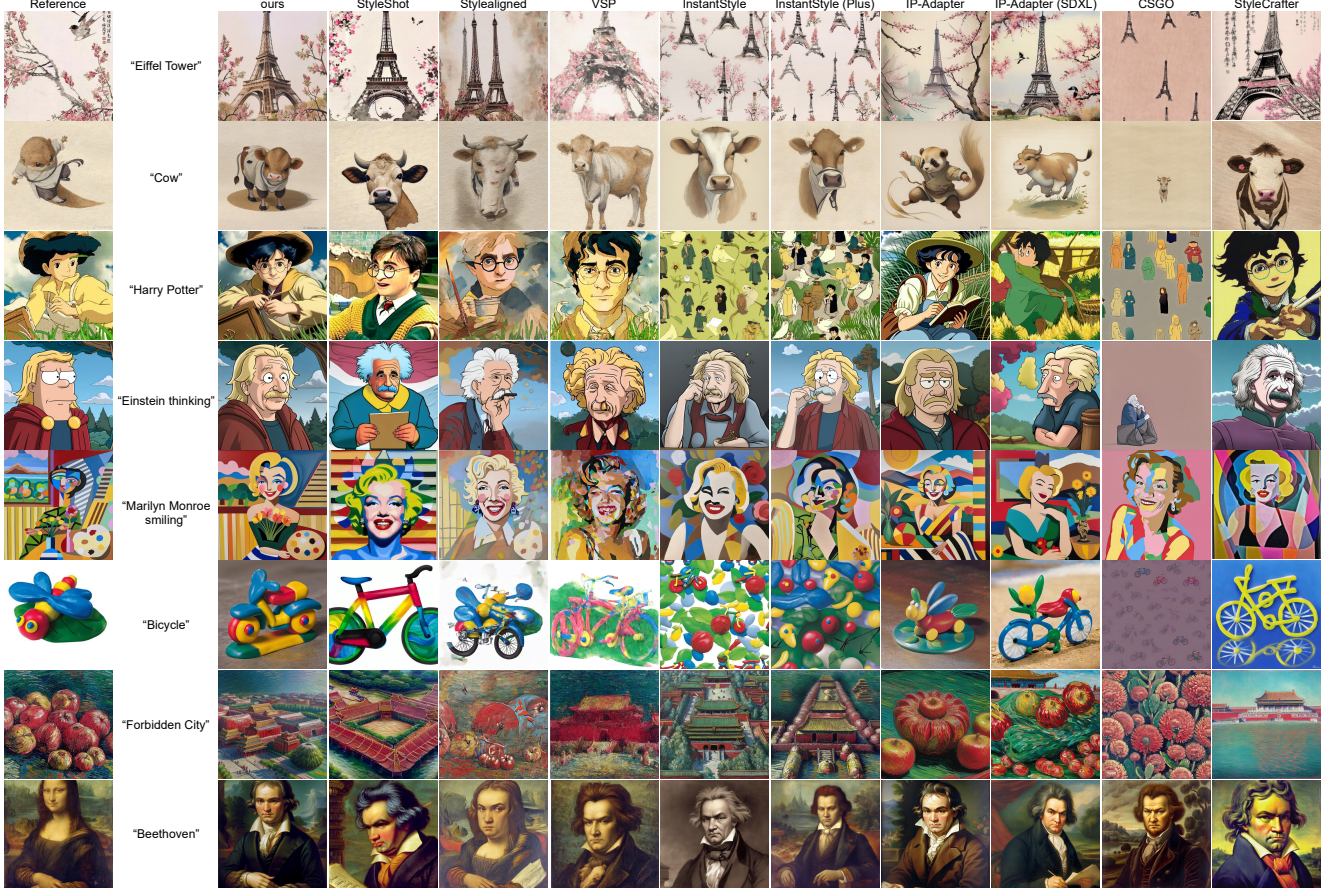


Figure 4. Qualitative comparison with other state-of-the-art text-guided stylization methods.

text prompt embeddings  $E_T$  to form the complete prompt embeddings for image generation:

$$E_P = E_T \oplus E_F, \quad (13)$$

where  $\oplus$  denotes the concatenation operation,  $E_P$  represents enhanced embeddings and integrates into the diffusion model. By balancing the above embeddings, the model gains a robust and controlled representation that captures multimodal conditions effectively, improving generation performance.

## 4. Experiments

### 4.1. Experimental Setup

We train ArtCrafter on a training data consisting of about 500,000 real image-text pairs from LAION-Aesthetic [36] and 50k art-text pairs from our proposed ArtMarket dataset. The images are paired with text descriptions generated by BLIP-2 [22], forming image-text data pairs. More explanations and examples of the data are given in the Supplementary Materials. During both training and inference, we resize the input images to a spatial resolution of  $512 \times 512$ . We

have implemented our method over [37] diffusion model. Our training processes are conducted using 8 NVIDIA A100 GPUs, each with 80GB of memory, and a batch size of 8 per GPU. The inference phase, which consumes 5185 MiB of memory, takes about one second of sampling time on a single A100 at denoising steps of 50.

### 4.2. Qualitative Evaluations

We evaluate our proposed method by comparing it with various existing methods, including but not limited to StyleShot [10], Style Aligned [13], VSP [19], InstantStyle [42], InstantStyle (Plus) [29, 42], IP-Adapter [48], IP-Adapter (SDXL) [29, 48], CSGO [46], and StyleCrafter [25]. We utilized the publicly available implementations of these methods and followed their recommended configurations for testing.

The qualitative comparison presented in Fig. 4 offers a visual assessment of the results achieved by various stylization methods. StyleShot shows some deficiencies in style representation, particularly in the capture of details and the consistency of style. Style Aligned and VSP sometimes exhibit discrepancies between the output style and the input style reference, which may lead to the loss of stylistic fea-

Metric	Ours	Stylerhot	Style Aligned	VSP	InstantSt.	InstantSt. (Plus)	IP-Ada.	IP-Ada. (SDXL)	CSGO	StyleCrafter
CLIP-Text $\uparrow$	<b>22.57</b>	22.46	18.26	22.29	19.78	19.53	15.01	19.14	17.82	19.37
CLIP-Image $\uparrow$	<b>69.48</b>	59.47	63.82	66.31	62.59	64.65	<u>68.90</u>	67.43	55.16	58.68
DINO-v2 $\uparrow$	<b>40.92</b>	23.45	27.89	35.34	29.76	30.62	<u>38.12</u>	32.98	24.53	31.60
LPIPS $\uparrow$	<b>0.4908</b>	<u>0.4561</u>	0.3892	0.2653	0.1478	0.1234	0.3456	0.2987	0.3655	0.3194
Human-Text $\uparrow$	/	38.89%	35.19%	30.56%	27.78%	24.07%	16.67%	13.89%	11.11%	10.19%
Human-Image $\uparrow$	/	35.19%	15.74%	40.74%	29.63%	25.00%	19.44%	21.30%	12.96%	32.41%
Human-Overall $\uparrow$	/	36.11%	18.52%	37.96%	14.81%	12.04%	22.22%	26.85%	9.26%	33.33%

Table 1. Quantitative comparison. The metrics employed for testing encompass image consistency (including CLIP-Image, DINO-v2, Human-Image), text consistency (CLIP-Text, Human-Text), diversity (LPIPS), and overall quality (Human-Overall) quality.

tures. Because the stylistic and semantic information in the style map is not completely separated, InstantStyle and its plus version deliver repeated non-essential semantic information in the results, such as the “Harry Potter” and “Bicycle” examples. The content information in the style image also affects the IP-Adapter and its SDXL version; for instance, the “apple” content is introduced in the “Forbidden City, Beijing” case. The fidelity of the results generated by CSGO is constrained by the number of art datasets. StyleCrafter produces outputs that are more consistent with the text, although the styles differ substantially from the reference image. As illustrated in Fig. 4, our method achieves captivating stylization by effectively transferring style patterns (such as brush strokes and lines). These style patterns are skillfully adapted to the content semantics, as seen in rows 1, 3, and 7 of Fig. 4.

### 4.3. Quantitative Evaluations

**Metric Description.** To comprehensively assess the quality of the models, we computed the following metrics: **CLIP-Text** [31] measures the textual consistency of the generated image with the target description by calculating the cosine similarity between the target caption and the generated image. **CLIP-Image** [31] evaluates the similarity of the generated image to the target style by calculating the cosine similarity between the target styling image and the generated image. **DINO-v2** [28] further verifies the style consistency of the generated image with the target style by calculating the feature similarity between the target style image and the generated image. **LPIPS** [51] measures the perceived similarity between two generated images, with higher values indicating less image similarity and better diversity.

As shown in Table 1, our method outperformed other text-guided stylization methods in the CLIP-Text, CLIP-Image, DINO-v2, and LPIPS metrics. This indicates that our method has a significant advantage in generating images that are highly consistent with the target description and style. Moreover, our method effectively retains the details and semantics of the content while maintaining high stylization quality as well as diversity.

Configuration	CLIP-Text $\uparrow$	CLIP-Image $\uparrow$	DINO-v2 $\uparrow$	LPIPS $\uparrow$
W.O. Sec. 3.2	23.49	66.81	37.25	0.4971
W.O. Sec. 3.3	19.13	70.52	41.77	0.4316
W.O. Sec. 3.4	22.19	71.39	42.63	0.3572

Table 2. Quantitative ablation study of proposed components.

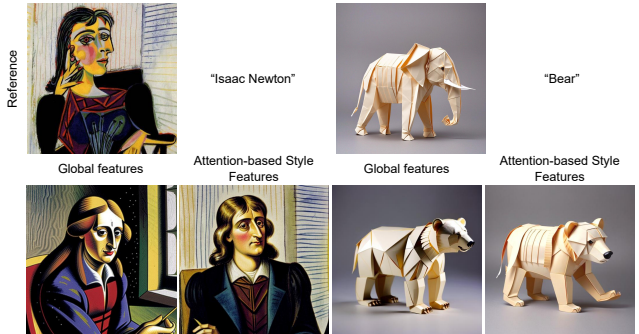


Figure 5. Visual differences between ArtCrafter generated samples with global features and attention-based style features.

### 4.4. User Study

To obtain a more comprehensive assessment, we conducted a user study. We randomly selected 30 generated results for each method covering a wide range of styles and hired 26 professionals in the art field to evaluate these generated results. Specifically, they rated text and image consistency on a scale of 1 – 5, resulting in the Human-Text and Human-Image scores in Table 1. The images with the best overall results are then pulled out to obtain the Human-Overall percentage results. The results in rows 6 – 8 of Table 1 indicate that the results generated by our proposed ArtCrafter are more favored in all three aspects. We notice the difference between objective evaluation metrics and subjective evaluation metrics because the former assesses each aspect in isolation. Whereas users may integrate information across various aspects, despite separate options provided. Human Preference suggests that our generated results have struck a better balance among text consistency, image consistency, and overall visual appeal.

### 4.5. Ablation Study

**quantitative analysis.** To fully evaluate the performance of the proposed components, we conduct an ablation

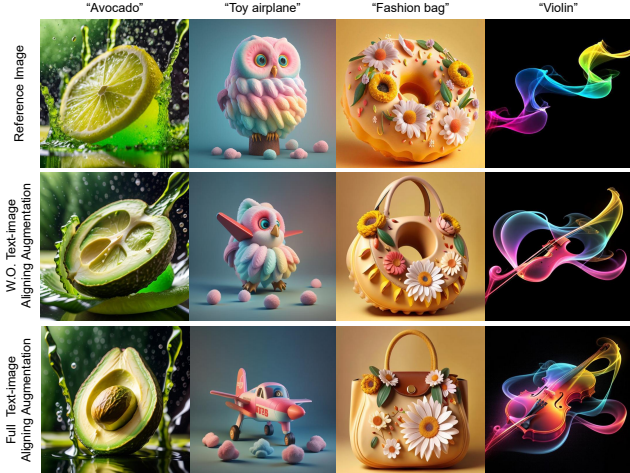


Figure 6. Ablation studies for text-image aligning augmentation. All results use the same seed as well as setup factors. From the results at the bottom of the figure, it can be observed that this component plays a key role in the function of text conditioning.

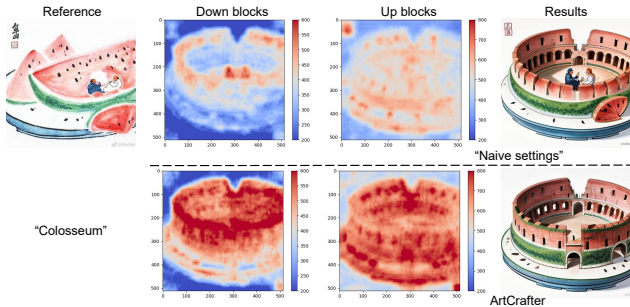


Figure 7. Ablation studies for text-image aligning augmentation. Results of the “Naive setting” show a tendency to favor the reference image content over the textual content and fail to adequately reconstruct the target content. With the addition of the text-image aligning augmentation module (bottom), the rearranged attention enables more favorable text-based content reconstruction.

study using both quantitative and qualitative methods. Table 2 summarizes the quantitative results, in which we test ArtCrafter’s performance after removing each essential technique component individually. Specifically, the metrics of CLIP-Text show that the attention-based style extraction component significantly enhances image consistency. Meanwhile, the evaluation results of CLIP-Image demonstrate that the text-image aligning augmentation component plays a positive role in guiding the text content. In addition, the results of measuring the similarity between the generated results using LPIPS indicate that the explicit modulation component plays a key role in enhancing the diversity of the generated results. Together, these findings demonstrate the significance and efficacy of the separate components in the entire strategy.

**Visualization analysis.** We first analyze the specific impact of attention-based style extraction (Sec. 3.2) on the results,

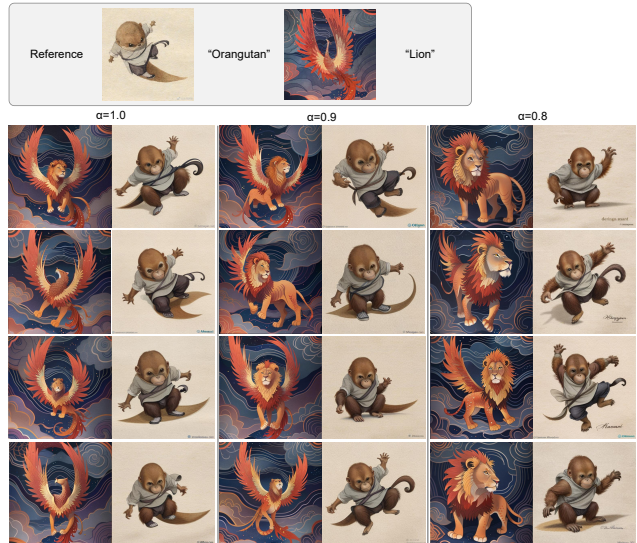


Figure 8. The effect of varying degrees of explicit modulation. As  $\alpha$  is increased, more varied results can be obtained (right columns), with some styles of misalignment of details.

as shown in Fig. 5. By utilizing this component, we effectively capture more detailed style features (e.g., line textures on walls and paper materials), thus achieving greater accuracy and richness in the style transfer process.

To evaluate the effectiveness of text-image aligning augmentation (Sec. 3.3), we provide a visual representation of the stylization results in Fig. 6 and Fig. 7. Fig. 6 demonstrates that the text-image aligning augmentation component effectively contributes to the efficacy of the text role. In addition, the heatmap in Fig. 7 reveals the cosine similarity between the cross-attention of the generated results and the textual self-attention results, suggesting that ArtCrafter, through a fine-grained setting of the attention mechanism, makes the generated images more compatible with what the text describes. This visual evidence supports the success of our strategy for achieving tighter compatibility and refinement between text and images via text-image aligning augmentation module.

Finally, we observe the effect of dynamic scale  $\alpha$  in explicit modulation (Sec. 3.4) on the diversity of the generated results by adjusting it. As shown in Fig. 8, increasing its effect produces a more diverse set of images, but it still shares common stylistic attributes with the reference image. We typically set  $\alpha$  to 0.8.

**Dataset.** We construct the ArtMarket dataset using art images from WikiArt [7] and LAION-Aesthetics [21], and BLIP-2 [22] as the textual style descriptive model to build the art-description data pairs. We perform the ablation study by training the model on the LAION-Aesthetics dataset. Fig. 9 shows that the model trained only on LAION-Aesthetics is more inclined to generate realistic style landscape images, while our trained model effectively generates

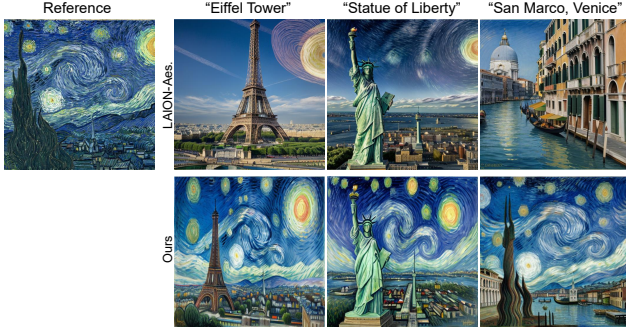


Figure 9. Visualization results of ArtCrafter architecture trained under different datasets respectively.



Figure 10. The visual presentations of the pre-trained diffusion model influenced by ArtCrafter at varying intensities.

the style of Van Gogh’s *Starry Night*. This demonstrates that incorporating artistic data improves the model’s performance in capturing artistic styles.

#### 4.6. Additional Analysis

**ArtCrafter control.** We test the role of ArtCrafter in the pre-training diffusion model. The result of adjusting the scale of ArtCrafter enhanced embedding  $E_{textP}$  in the pre-trained diffusion model is shown in Fig. 10. In this work, we usually set the scale to 0.6 to balance content and style. This verifies that ArtCrafter can effectively enhance the applicability of pre-trained diffusion models in the art generation domain at a lower training cost. With this adjustment, we can more flexibly control the degree of text consistency and stylization of the generated images to meet different creative needs.

**ArtCrafter with additional conditions applied.** Benefiting from our design without any changes to the network structure of the original diffusion model, ArtCrafter is seamlessly compatible with existing controllable tools [50]. Fig. 11 shows the diverse examples generated by applying different structural controls, including canny edge detection [3], normal map [40], HED edge detection [45], linear edge, and MiDaS depth map [32]. These examples not only highlight ArtCrafter’s flexibility in adapting to a variety of conditions but also foretell its great potential for application in the 3D field, opening up new possibilities for artistic creation and visual design.

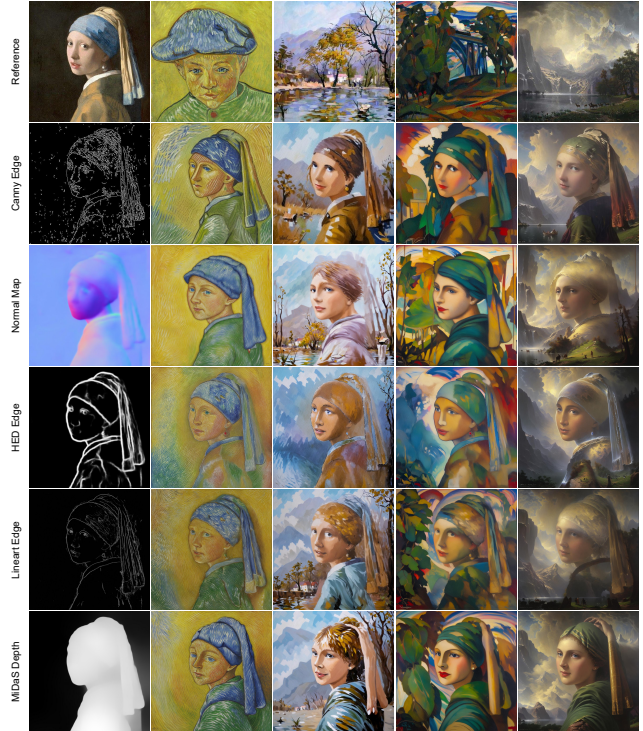


Figure 11. The combination of ArtCrafter and additional conditions. The results of this combination show that ArtCrafter can accept images as content guidance, achieve style transfer effects, and be compatible with 3D content information.

## 5. Conclusion

In this paper, we introduce ArtCrafter, a novel text-image aligning style transfer framework achieved through an embedding reframing architecture. Our approach ensures superior text-guided style transfer quality by integrating three core components: attention-based style extraction, text-image aligning augmentation, and explicit modulation. Comprehensive evaluations demonstrate ArtCrafter strengths in adapting to diverse artistic styles, maintaining textual prompt consistency, enhancing output diversity, and improving overall visual quality.

Acknowledging the current limitations of our work, for future research, we intend to enhance our approach by incorporating pattern reproducibility and contextual elements within style images, including the relative positioning of style patches, to facilitate a more cohesive art style transfer. We expect that advancements in the extraction and fusion of style and content features, coupled with an investigation into the method’s scalability and adaptability, will markedly enhance the quality of style transfer and provide more precise control over the shape and appearance similarity of the generated images.



## References

- [1] Omri Avrahami, Dani Lischinski, and Ohad Fried. Blended diffusion for text-driven editing of natural images. In *Proceedings of the IEEE/CVF Conference on Computer Vision and Pattern Recognition*, pages 18208–18218, 2022. 2
- [2] Tim Brooks, Aleksander Holynski, and Alexei A Efros. Instructpix2pix: Learning to follow image editing instructions. In *Proceedings of the IEEE/CVF Conference on Computer Vision and Pattern Recognition*, pages 18392–18402, 2023. 2
- [3] John Canny. A computational approach to edge detection. *IEEE Transactions on Pattern Analysis and Machine Intelligence*, (6):679–698, 1986. 8
- [4] Mingdeng Cao, Xintao Wang, Zhongang Qi, Ying Shan, Xiaohu Qie, and Yinqiang Zheng. Masactrl: Tuning-free mutual self-attention control for consistent image synthesis and editing. In *Proceedings of the IEEE/CVF International Conference on Computer Vision*, pages 22560–22570, 2023. 2
- [5] Dar-Yen Chen, Hamish Tennent, and Ching-Wen Hsu. Artadapter: Text-to-image style transfer using multi-level style encoder and explicit adaptation. In *Proceedings of the IEEE/CVF Conference on Computer Vision and Pattern Recognition*, pages 8619–8628, 2024. 1
- [6] Jiwoo Chung, Sangeek Hyun, and Jae-Pil Heo. Style injection in diffusion: A training-free approach for adapting large-scale diffusion models for style transfer. In *Proceedings of the IEEE/CVF Conference on Computer Vision and Pattern Recognition*, pages 8795–8805, 2024. 1, 2
- [7] Wikiart Contributors. Wikiart website, 2024. 7, 2
- [8] Yingying Deng, Xiangyu He, Fan Tang, and Weiming Dong. Z\*: Zero-shot style transfer via attention reweighting. In *Proceedings of the IEEE/CVF Conference on Computer Vision and Pattern Recognition*, pages 6934–6944, 2024. 1, 3
- [9] Prajwal Ganugula, Y S S S Santosh Kumar, N K Sagar Reddy, Prabhath Chellingi, Avinash Thakur, Neeraj Kasera, and C Shyam Anand. Mosaic: Multi-object segmented arbitrary stylization using clip. In *Proceedings of the IEEE/CVF International Conference on Computer Vision Workshops*, pages 892–903, 2023. 3
- [10] Junyao Gao, Yanchen Liu, Yanan Sun, Yinhao Tang, Yanhong Zeng, Kai Chen, and Cairong Zhao. Styleshot: A snapshot on any style. *arXiv preprint arXiv:2407.01414*, 2024. 2, 3, 5
- [11] Yue Han, Junwei Zhu, Keke He, Xu Chen, Yanhao Ge, Wei Li, Xiangtai Li, Jiangning Zhang, Chengjie Wang, and Yong Liu. Face adapter for pre-trained diffusion models with fine-grained id and attribute control. *arXiv preprint arXiv:2405.12970*, 2024. 2
- [12] Amir Hertz, Ron Mokady, Jay Tenenbaum, Kfir Aberman, Yael Pritch, and Daniel Cohen-Or. Prompt-to-prompt image editing with cross attention control. 2022. 2
- [13] Amir Hertz, Andrey Voynov, Shlomi Fruchter, and Daniel Cohen-Or. Style aligned image generation via shared attention. In *Proceedings of the IEEE/CVF Conference on Computer Vision and Pattern Recognition*, pages 4775–4785, 2024. 3, 5
- [14] Jonathan Ho, Ajay Jain, and Pieter Abbeel. Denoising diffusion probabilistic models. *Advances in Neural Information Processing Systems*, 33:6840–6851, 2020. 2
- [15] Mengqi Huang, Zhendong Mao, Mingcong Liu, Qian He, and Yongdong Zhang. Realcustom: Narrowing real text word for real-time open-domain text-to-image customization. In *Proceedings of the IEEE/CVF Conference on Computer Vision and Pattern Recognition*, pages 7476–7485, 2024. 1
- [16] Nisha Huang, Weiming Dong, Yuxin Zhang, Fan Tang, Ronghui Li, Chongyang Ma, Xiu Li, and Changsheng Xu. Creativesynth: Creative blending and synthesis of visual arts based on multimodal diffusion. *arXiv preprint arXiv:2401.14066*, 2024. 1
- [17] Nisha Huang, Yuxin Zhang, Fan Tang, Chongyang Ma, Haibin Huang, Weiming Dong, and Changsheng Xu. Diffstyler: Controllable dual diffusion for text-driven image stylization. *IEEE Transactions on Neural Networks and Learning Systems*, 2024. 2
- [18] Andrew Jaegle, Felix Gimeno, Andy Brock, Oriol Vinyals, Andrew Zisserman, and Joao Carreira. Perceiver: General perception with iterative attention. In *International Conference on Machine Learning*, pages 4651–4664. PMLR, 2021. 4
- [19] Jaeseok Jeong, Junho Kim, Yunje Choi, Gayoung Lee, and Youngjung Uh. Visual style prompting with swapping self-attention. *arXiv preprint arXiv:2402.12974*, 2024. 3, 5
- [20] Ruixiang Jiang, Can Wang, Jingbo Zhang, Menglei Chai, Mingming He, Dongdong Chen, and Jing Liao. Avatarcraft: Transforming text into neural human avatars with parameterized shape and pose control. In *Proceedings of the IEEE/CVF International Conference on Computer Vision*, pages 14371–14382, 2023. 1
- [21] LAION-AI. LAION-Aesthetics V1. Technical report, LAION-AI, 2024. 7, 2
- [22] Junnan Li, Dongxu Li, Silvio Savarese, and Steven Hoi. Blip-2: Bootstrapping language-image pre-training with frozen image encoders and large language models. In *International Conference on Machine Learning*, pages 19730–19742. PMLR, 2023. 5, 7, 2
- [23] Zhen Li, Mingdeng Cao, Xintao Wang, Zhongang Qi, Mingming Cheng, and Ying Shan. Photomaker: Customizing realistic human photos via stacked id embedding. In *Proceedings of the IEEE/CVF Conference on Computer Vision and Pattern Recognition*, pages 8640–8650, 2024. 1
- [24] Kuan Heng Lin, Sicheng Mo, Ben Klingher, Fangzhou Mu, and Bolei Zhou. Ctrl-x: Controlling structure and appearance for text-to-image generation without guidance. *arXiv preprint arXiv:2406.07540*, 2024. 2
- [25] Gongye Liu, Menghan Xia, Yong Zhang, Haoxin Chen, Jinbo Xing, Xintao Wang, Yujiu Yang, and Ying Shan. Stylecrafter: Enhancing stylized text-to-video generation with style adapter. *arXiv preprint arXiv:2312.00330*, 2023. 2, 3, 5
- [26] Zhi-Song Liu, Li-Wen Wang, Wan-Chi Siu, and Vicky Kalogeiton. Name your style: text-guided artistic style transfer. In *Proceedings of the IEEE/CVF Conference on Computer Vision and Pattern Recognition*, pages 3530–3534, 2023. 3

- [27] Jian Ma, Junhao Liang, Chen Chen, and Haonan Lu. Subject-diffusion: Open domain personalized text-to-image generation without test-time fine-tuning. In *ACM SIGGRAPH 2024 Conference Papers*, pages 1–12, 2024. 1
- [28] Maxime Oquab, Timothée Darcet, Theo Moutakanni, Huy V. Vo, Marc Szafraniec, Vasil Khalidov, Pierre Fernandez, Daniel Haziza, Francisco Massa, Alaaeldin El-Nouby, Russell Howes, Po-Yao Huang, Hu Xu, Vasu Sharma, Shangwen Li, Wojciech Galuba, Mike Rabbat, Mido Assran, Nicolas Ballas, Gabriel Synnaeve, Ishan Misra, Herve Jegou, Julien Mairal, Patrick Labatut, Armand Joulin, and Piotr Bojanowski. Dinov2: Learning robust visual features without supervision, 2023. 6
- [29] Dustin Podell, Zion English, Kyle Lacey, Andreas Blattmann, Tim Dockhorn, Jonas Müller, Joe Penna, and Robin Rombach. Sdxl: Improving latent diffusion models for high-resolution image synthesis. *arXiv preprint arXiv:2307.01952*, 2023. 1, 2, 5
- [30] Tianhao Qi, Shancheng Fang, Yanze Wu, Hongtao Xie, Jiawei Liu, Lang Chen, Qian He, and Yongdong Zhang. Deadiff: An efficient stylization diffusion model with disentangled representations. In *Proceedings of the IEEE/CVF Conference on Computer Vision and Pattern Recognition*, pages 8693–8702, 2024. 3
- [31] Alec Radford, Jong Wook Kim, Chris Hallacy, Aditya Ramesh, Gabriel Goh, Sandhini Agarwal, Girish Sastry, Amanda Askell, Pamela Mishkin, Jack Clark, et al. Learning transferable visual models from natural language supervision. In *International Conference on Machine Learning*, pages 8748–8763. PMLR, 2021. 4, 6, 2
- [32] René Ranftl, Katrin Lasinger, David Hafner, Konrad Schindler, and Vladlen Koltun. Towards robust monocular depth estimation: Mixing datasets for zero-shot cross-dataset transfer. *IEEE Transactions on Pattern Analysis and Machine Intelligence*, 44(3):1623–1637, 2020. 8
- [33] Robin Rombach, Andreas Blattmann, Dominik Lorenz, Patrick Esser, and Björn Ommer. High-resolution image synthesis with latent diffusion models. In *Proceedings of the IEEE/CVF Conference on Computer Vision and Pattern Recognition*, pages 10684–10695, 2022. 1, 2, 3
- [34] Olaf Ronneberger, Philipp Fischer, and Thomas Brox. U-net: Convolutional networks for biomedical image segmentation. In *Medical Image Computing and Computer-Assisted Intervention*, pages 234–241. Springer, 2015. 3
- [35] Ciara Rowles, Shimon Vainer, Dante De Nigris, Slava Elizarov, Konstantin Kutsy, and Simon Donné. Ipadapter-instruct: Resolving ambiguity in image-based conditioning using instruct prompts. *arXiv preprint arXiv:2408.03209*, 2024. 2
- [36] Christoph Schuhmann, Romain Beaumont, Richard Vencu, Cade Gordon, Ross Wightman, Mehdi Cherti, Theo Coombes, Aarush Katta, Clayton Mullis, Mitchell Wortsman, et al. Laion-5b: An open large-scale dataset for training next generation image-text models. *Advances in Neural Information Processing Systems*, 35:25278–25294, 2022. 5
- [37] SG161222. Realistic-vision-v4.0-novae, 2024. 3, 5
- [38] Jaskirat Singh, Stephen Gould, and Liang Zheng. High-fidelity guided image synthesis with latent diffusion models. In *2023 IEEE/CVF Conference on Computer Vision and Pattern Recognition*, pages 5997–6006. IEEE, 2023. 2
- [39] Kihyuk Sohn, Lu Jiang, Jarred Barber, Kimin Lee, Nataniel Ruiz, Dilip Krishnan, Huiwen Chang, Yuanzhen Li, Irfan Essa, Michael Rubinstein, et al. Styledrop: Text-to-image synthesis of any style. *Advances in Neural Information Processing Systems*, 36, 2024. 3
- [40] Igor Vasiljevic, Nick Kolkin, Shanyi Zhang, Ruotian Luo, Haochen Wang, Falcon Z Dai, Andrea F Daniele, Mohammadreza Mostajabi, Steven Basart, Matthew R Walter, et al. Diode: A dense indoor and outdoor depth dataset. *arXiv preprint arXiv:1908.00463*, 2019. 8
- [41] A Vaswani. Attention is all you need. *Advances in Neural Information Processing Systems*, 2017. 4
- [42] Haofan Wang, Qixun Wang, Xu Bai, Zekui Qin, and Anthony Chen. Instantstyle: Free lunch towards style-preserving in text-to-image generation. *arXiv preprint arXiv:2404.02733*, 2024. 2, 3, 5
- [43] Jiangshan Wang, Yifan Pu, Yizeng Han, Jiayi Guo, Yiru Wang, Xiu Li, and Gao Huang. Gra: Detecting oriented objects through group-wise rotating and attention. *arXiv preprint arXiv:2403.11127*, 2024. 2
- [44] Qixun Wang, Xu Bai, Haofan Wang, Zekui Qin, Anthony Chen, Huaxia Li, Xu Tang, and Yao Hu. Instantid: Zero-shot identity-preserving generation in seconds. *arXiv preprint arXiv:2401.07519*, 2024. 1
- [45] Saining Xie and Zhuowen Tu. Holistically-nested edge detection. In *Proceedings of the IEEE International Conference on Computer Vision*, pages 1395–1403, 2015. 8
- [46] Peng Xing, Haofan Wang, Yanpeng Sun, Qixun Wang, Xu Bai, Hao Ai, Renyuan Huang, and Zechao Li. Csgo: Content-style composition in text-to-image generation. *arXiv preprint arXiv:2408.16766*, 2024. 2, 3, 5
- [47] Haibo Yang, Yang Chen, Yingwei Pan, Ting Yao, Zhineng Chen, and Tao Mei. 3dstyle-diffusion: Pursuing fine-grained text-driven 3d stylization with 2d diffusion models. In *Proceedings of the 31st ACM International Conference on Multimedia*, pages 6860–6868, 2023. 3
- [48] Hu Ye, Jun Zhang, Sibio Liu, Xiao Han, and Wei Yang. Ip-adapter: Text compatible image prompt adapter for text-to-image diffusion models. *arXiv preprint arXiv:2308.06721*, 2023. 2, 3, 5
- [49] Kai Zhang, Yawei Li, Wangmeng Zuo, Lei Zhang, Luc Van Gool, and Radu Timofte. Plug-and-play image restoration with deep denoiser prior. *IEEE Transactions on Pattern Analysis and Machine Intelligence*, 44(10):6360–6376, 2021. 2
- [50] Lvmin Zhang, Anyi Rao, and Maneesh Agrawala. Adding conditional control to text-to-image diffusion models. In *Proceedings of the IEEE/CVF International Conference on Computer Vision*, pages 3836–3847, 2023. 2, 8
- [51] Richard Zhang, Phillip Isola, Alexei A Efros, Eli Shechtman, and Oliver Wang. The unreasonable effectiveness of deep features as a perceptual metric. In *Proceedings of the IEEE/CVF Conference on Computer Vision and Pattern Recognition*, pages 586–595, 2018. 6
- [52] Yuxin Zhang, Nisha Huang, Fan Tang, Haibin Huang, Chongyang Ma, Weiming Dong, and Changsheng Xu.

Inversion-based style transfer with diffusion models. In *Proceedings of the IEEE/CVF Conference on Computer Vision and Pattern Recognition*, pages 10146–10156, 2023. [1](#)

- [53] Zhanjie Zhang, Quanwei Zhang, Wei Xing, Guangyuan Li, Lei Zhao, Jiakai Sun, Zehua Lan, Junsheng Luan, Yiling Huang, and Huaizhong Lin. Artbank: Artistic style transfer with pre-trained diffusion model and implicit style prompt bank. In *Proceedings of the AAAI Conference on Artificial Intelligence*, pages 7396–7404, 2024. [1](#)

# ArtCrafter: Text-Image Aligning Style Transfer via Embedding Reframing

## Supplementary Material

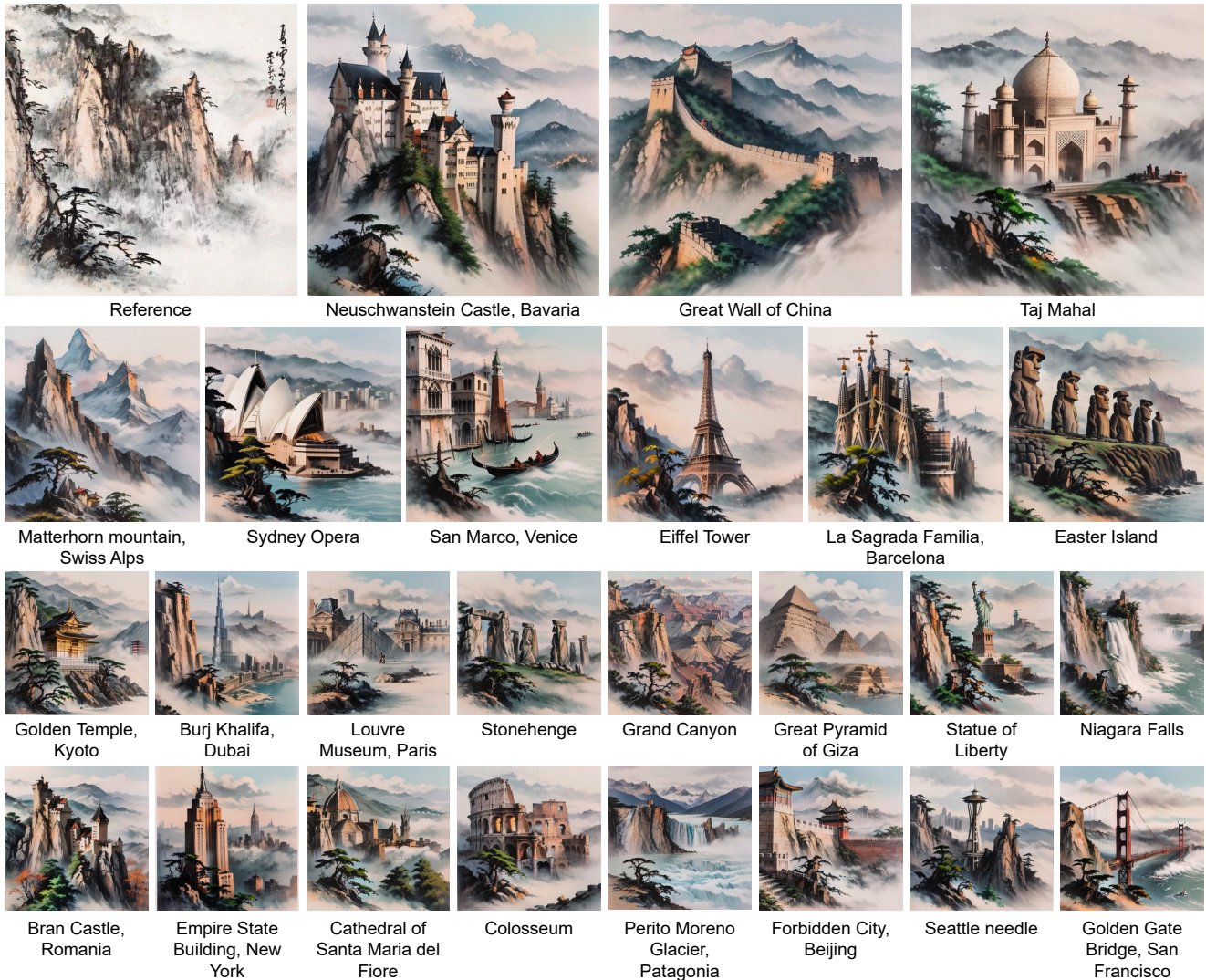


Figure 1. **ArtCrafter generation results.** By injecting the features of the reference images and text prompts during the diffusion process, our method is capable of capturing and generating a faithful style representation.

### A. Additional Results

Fig. 1 illustrates our approach to transferring the “ink painting” style from a reference image to iconic global landmarks. For the references, users need not include terms like “painting,” “art,” “ink painting,” or other explicit artistic descriptors; instead, they can input straightforward content descriptors, such as “Neuschwanstein Castle, Bavaria.” This simplifies the user’s interaction process. Furthermore, Figs 9, 10, 11, 12, 13, 14, 15, 16, and 17 display the style transfer effects on subjects including people, animals, and landscapes.

### B. Additional Comparisons

**Quantitative comparison.** In Fig. 2, we present an expanded set of comparative results with the current state-of-the-art methods, encompassing a diverse array of styles and textual inputs. These thorough comparative analyses underscore the robustness and superiority of ArtCrafter, showcasing its adept handling of varied styles and textual contents. The comparisons not only manifest ArtCrafter’s proficiency in executing style transfer efficiently but also accentuate its precision in preserving the integrity of text content.

**Quantitative comparison visualization.** In Fig. 3, we

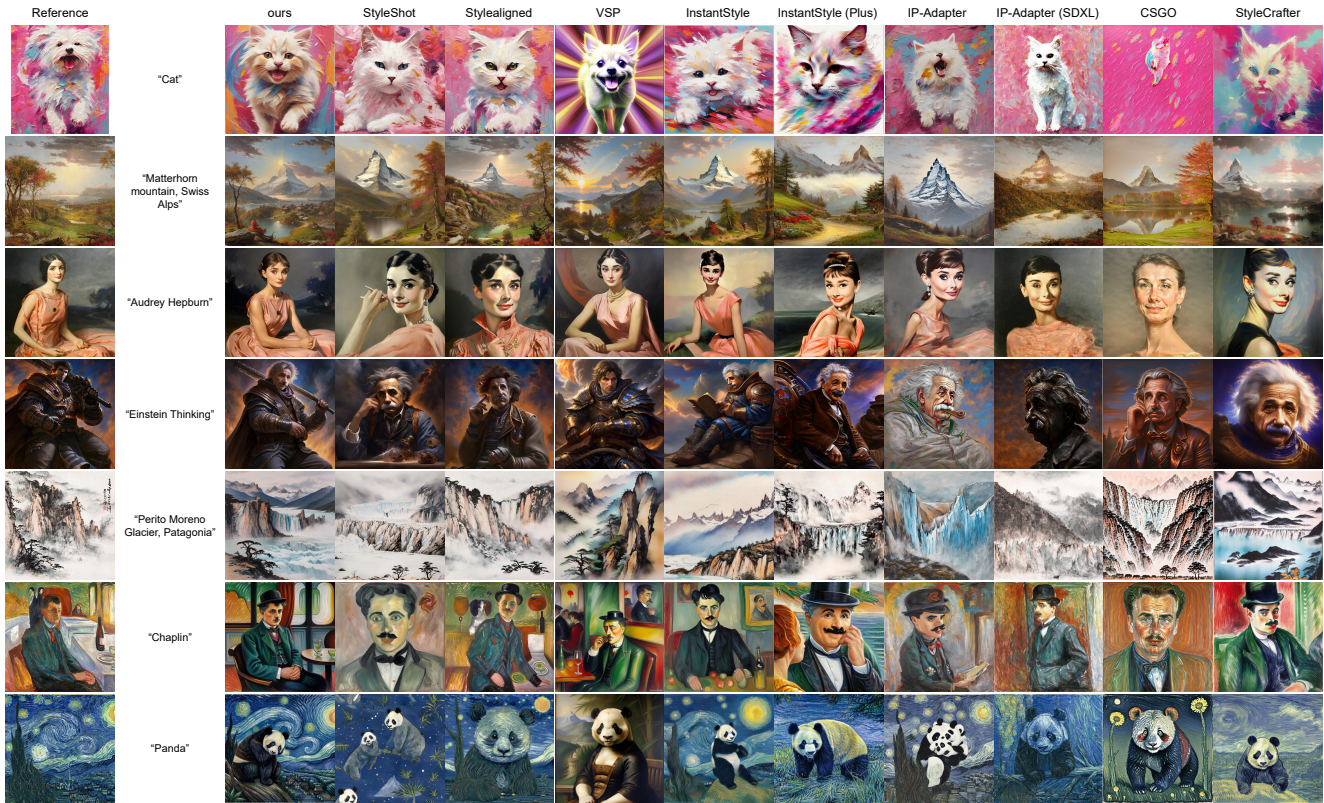


Figure 2. Additional qualitative comparison with other state-of-the-art text-guided stylization methods.

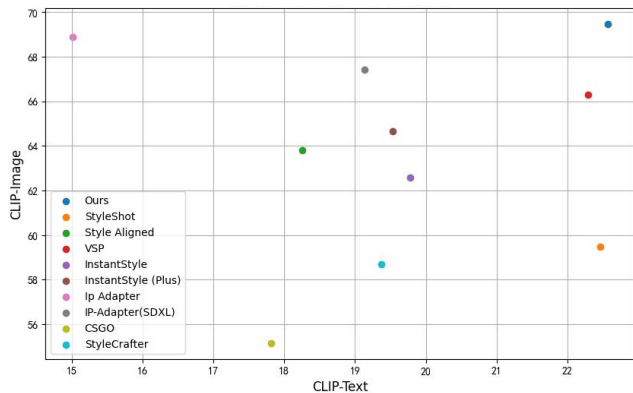


Figure 3. Quantitative comparison visualization.

employ scatter plots to visualize the performance of the state-of-the-art methods in terms of the quantitative metrics CLIP-Image [31] and CLIP-Text. This visualization effectively demonstrates how our method strikes a balance between stylistic and content expression, thereby showcasing its exceptional performance. By plotting the results on these metrics, we provide a clear and concise comparison that illustrates the strengths of ArtCrafter in achieving a harmonious blend of style and content, which is a critical aspect in the field of style transfer generation.

### C. ArtMarket Dataset

Our dataset, ArtMarket, depicted in Fig. 4, comprises a rich collection of artworks accompanied by their corresponding textual descriptions. The visual content of the dataset is primarily sourced from the extensive art repository of WikiArt [7] and LAION-Aesthetics [21], which features a diverse range of artistic styles and periods. The descriptive texts are derived from BLIP-2 [22], a sophisticated language model that provides detailed and contextually rich captions. This combination of high-quality images and descriptively accurate texts allows ArtMarket to effectively support the training of models aimed at style transfer and content generation in the realm of text-to-image synthesis.

### D. Additional Ablation Study

**Text-image aligning augmentation.** Fig. 5 presents an array of additional ablation study results for our text-image aligning augmentation component, underscoring its role in bolstering the efficacy of text-guided content generation. These results demonstrate that our component significantly enhances the model’s ability to produce content that aligns closely with the textual prompts, without compromising the stylistic integrity of the image. The experiments showcase how the integration of our aligning augmentation leads to a

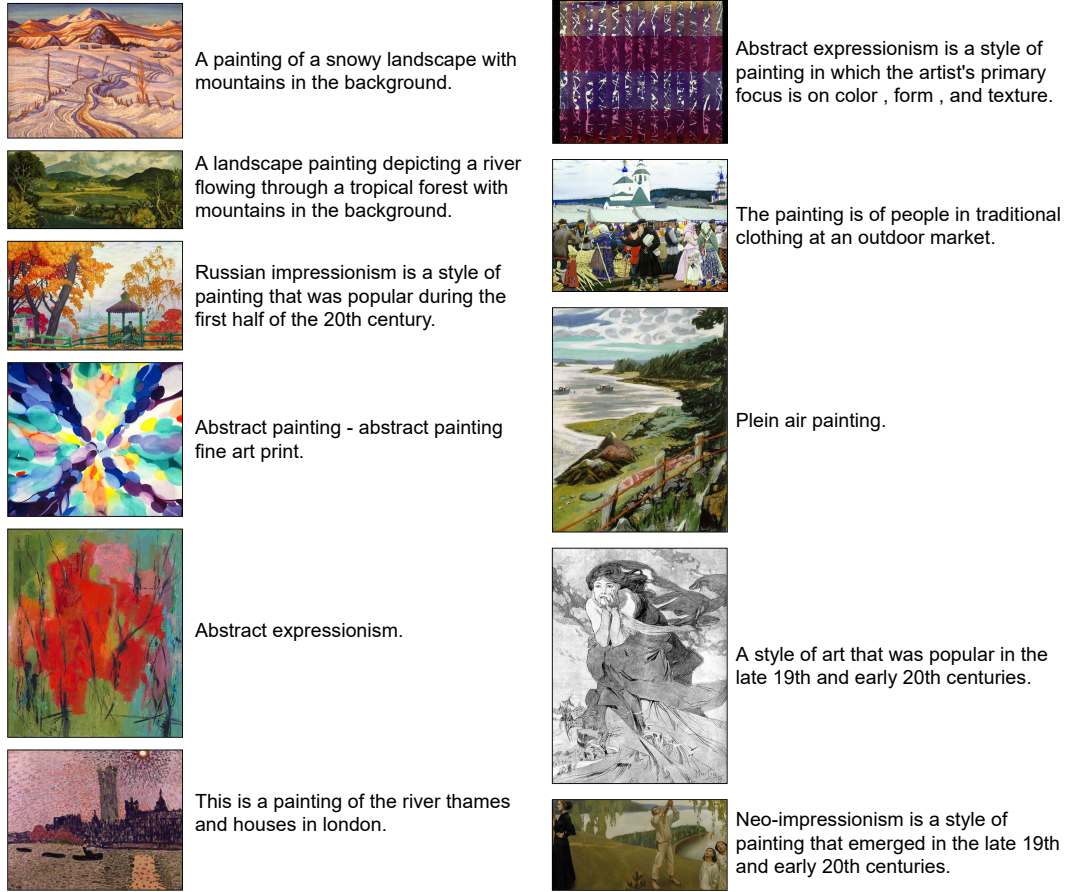


Figure 4. Dataset samples. A collection of artworks and corresponding textual descriptions.



Figure 5. Style transfer results with text-image aligning augmentation ablation study.

harmonious fusion of content fidelity and style preservation.

**Diversity.** Fig. 6 elaborates on the ablation study results for our Explicit Modulation component, further substantiating

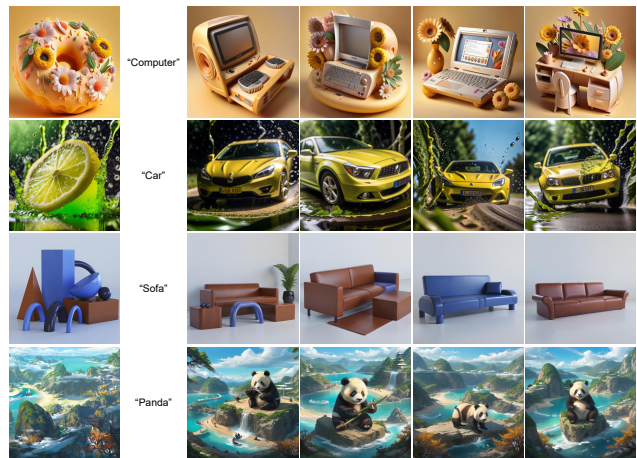


Figure 6. Diversity results with explicit modulation ablation study.

its effectiveness in augmenting the diversity of content generation. These results highlight the component's capacity to enrich the variety of outputs produced by the model, ensuring a broader spectrum of creative expressions. The experiments detailed in Fig. 6 underscore how explicit modulation

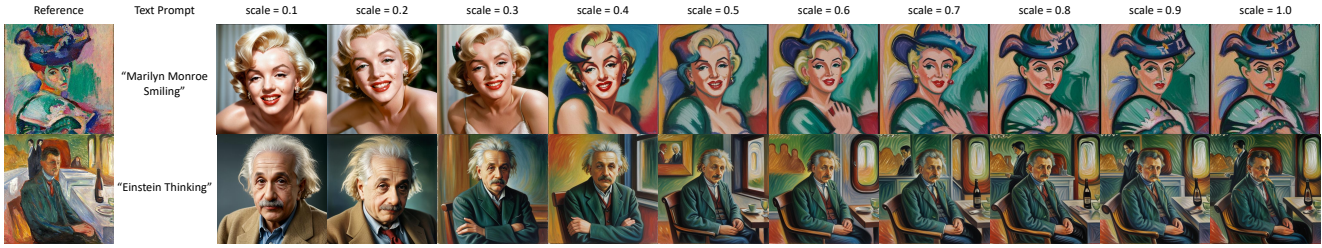


Figure 7. Ablation study of ArtCrafter guidance scale.

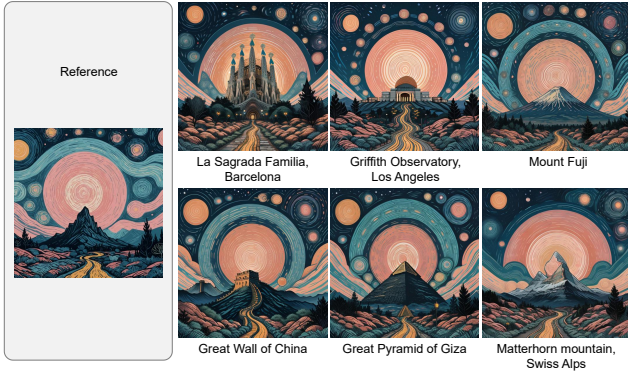


Figure 8. Failure cases. Instances of ineffective style transfer.

lead to more stable and faithful style transfers. Despite this, the overall effectiveness of our approach in handling complex style elements is evident.

contributes to the generation of images that not only capture the essence of the input text but also exhibit a wide range of artistic styles, thus validating its importance in achieving diverse and compelling visual outcomes.

**Guidance scale.** We conduct comprehensive validation of the integration of ArtCrafter composite modules into the U-Net structure of the diffusion model. This validation serves as a supplementary extension to the main experimental results presented in the text, offering an in-depth analysis of the model’s performance across a range of guidance intensities. Specifically, Fig. 7 illustrates the outcomes at intervals of 0.1 for the guidance coefficient, thereby providing a granular view of how varying levels of input influence the final generation quality. These additional results underscore the robustness and flexibility of ArtCrafter approach in adapting to different degrees of user-specified control.

## E. Failure Cases

Our work exhibits a degree of instability in consistently capturing the precise locations of distinctive stylistic textures, as depicted in Fig. 8. The reference images contain extensive, curved textural elements, exemplified by the blue and pink curves, which pose a significant challenge for our model to fully assimilate and reproduce in the generated outputs. This observation highlights an area for future improvement, where enhancing the model’s ability to accurately replicate intricate, long-range textural patterns could

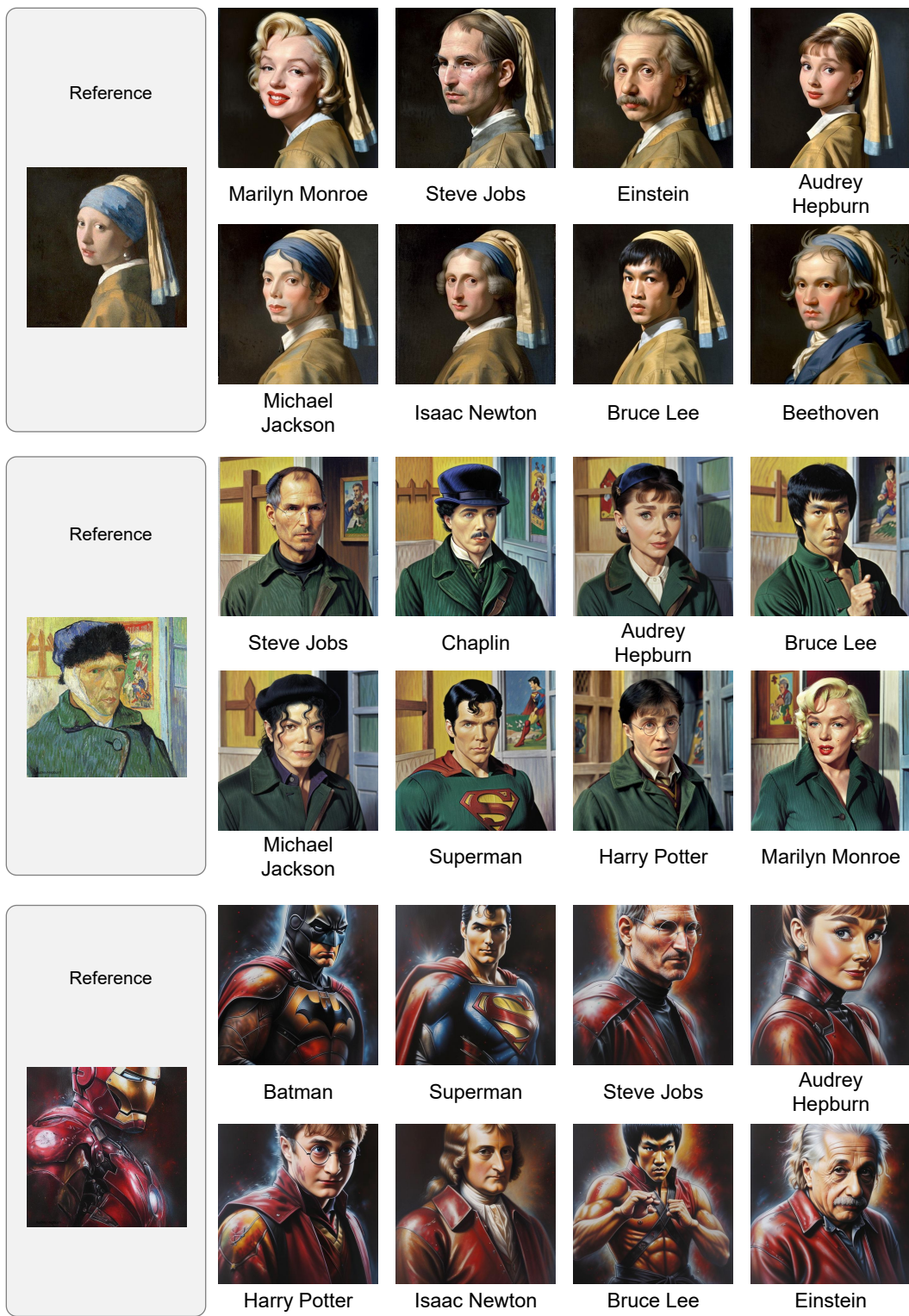


Figure 9. Additional results. Further demonstrations of style transfer efficacy.



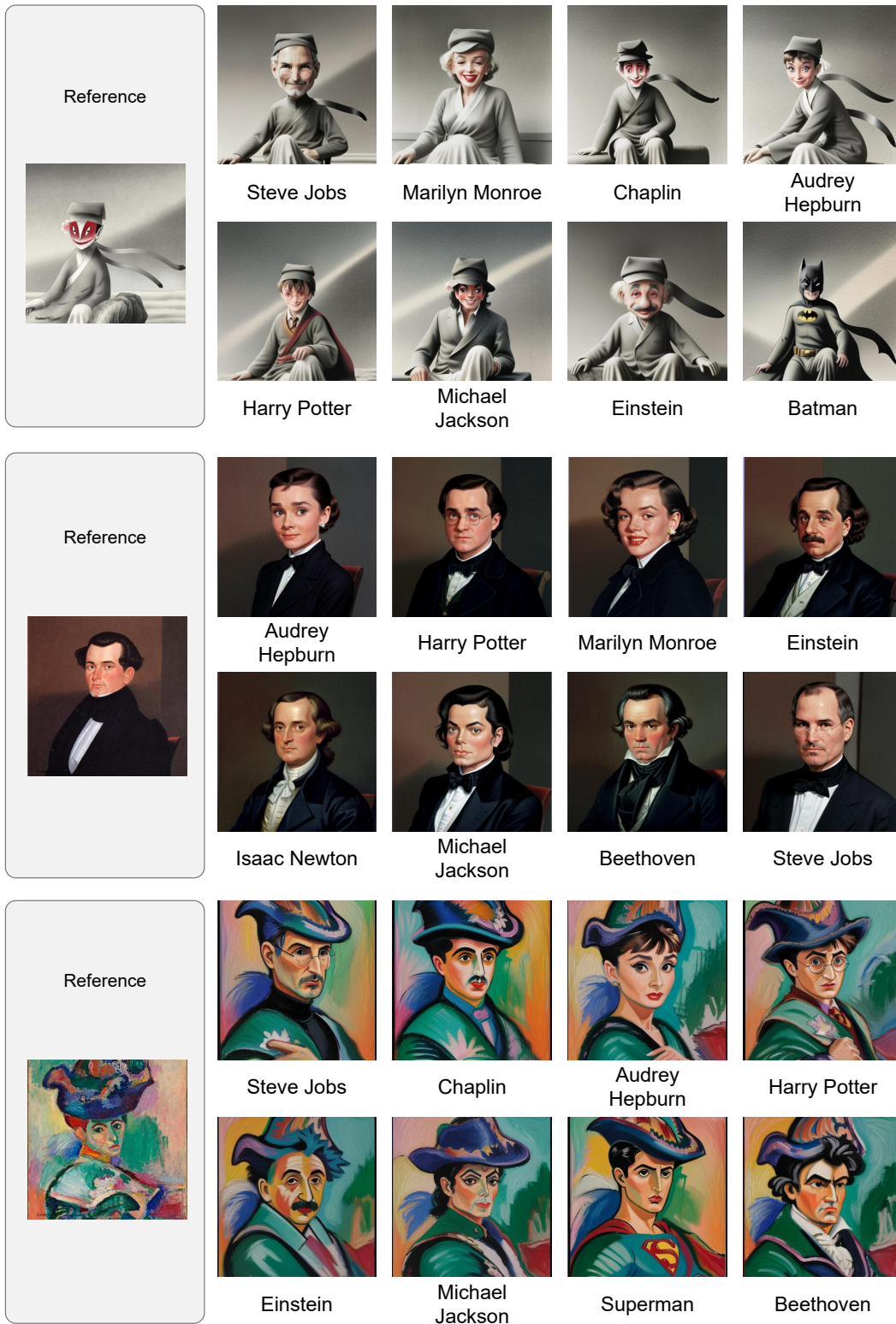
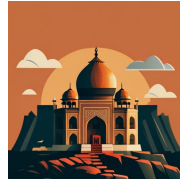


Figure 10. Additional results. Further demonstrations of style transfer efficacy.

Reference



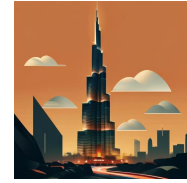
Sydney Opera



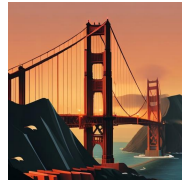
Taj Mahal



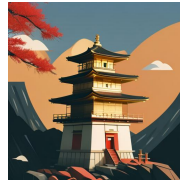
Bran Castle  
(Dracula's  
Castle),  
Romania



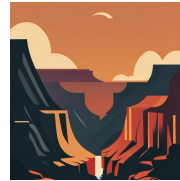
Burj Khalifa,  
Dubai



Golden Gate  
Bridge, San  
Francisco



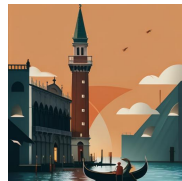
Golden Temple,  
Kyoto



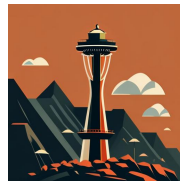
Grand Canyon



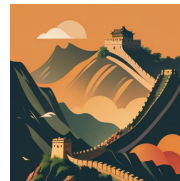
Great Pyramid  
of Giza



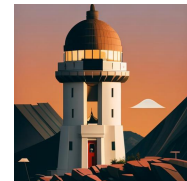
San Marco,  
Venice



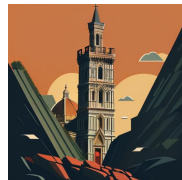
Seattle needle



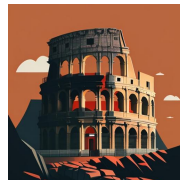
Great Wall of  
China



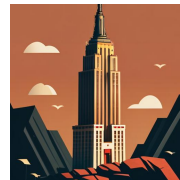
Griffith  
Observatory,  
Los Angeles



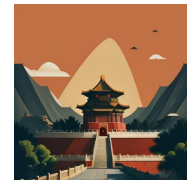
Cathedral of  
Santa Maria del  
Fiore



Colosseum



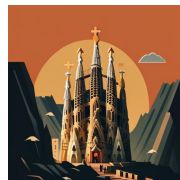
Empire State  
Building, New  
York



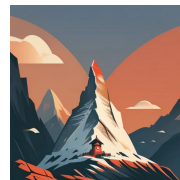
Forbidden City,  
Beijing



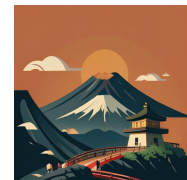
Niagara Falls



La Sagrada  
Familia,  
Barcelona



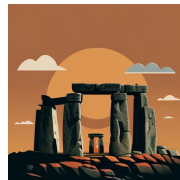
Matterhorn  
mountain,  
Swiss Alps



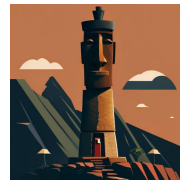
Mount Fuji



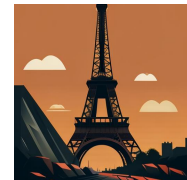
Statue of  
Liberty



Stonehenge



Easter Island



Eiffel Tower

Figure 11. Additional results. Further demonstrations of style transfer efficacy.



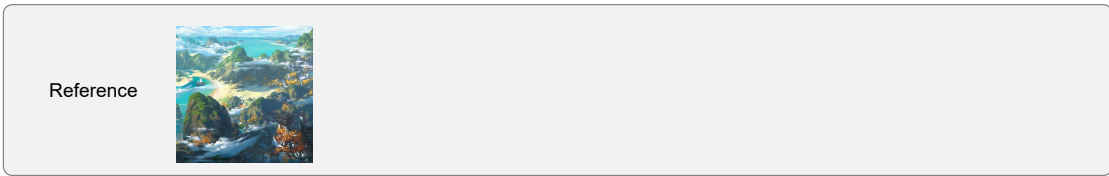
Matterhorn mountain, Swiss Alps    Neuschwanstein Castle, Bavaria    Niagara Falls    San Marco, Venice    Statue of Liberty    Stonehenge    Sydney Opera    Taj Mahal



Aurora, Norway Fjords    Burj Khalifa, Dubai    Cathedral of Santa Maria del Fiore    Colosseum    Easter Island    Eiffel Tower    Empire State Building, New York    Forbidden City, Beijing



Golden Gate Bridge, San Francisco    Golden Temple, Kyoto    Grand Canyon    Great Pyramid of Giza    Great Wall of China    Griffith Observatory, Los Angeles    La Sagrada Familia, Barcelona    Louvre Museum, Paris



Taj Mahal    Sydney Opera    Bran Castle (Dracula's Castle), Romania    Burj Khalifa, Dubai    Cathedral of Santa Maria del Fiore    Colosseum    Easter Island    Stonehenge



Eiffel Tower    Empire State Building, New York    Forbidden City, Beijing    Golden Gate Bridge, San Francisco    Golden Temple, Kyoto    Grand Canyon    Great Pyramid of Giza    Great Wall of China

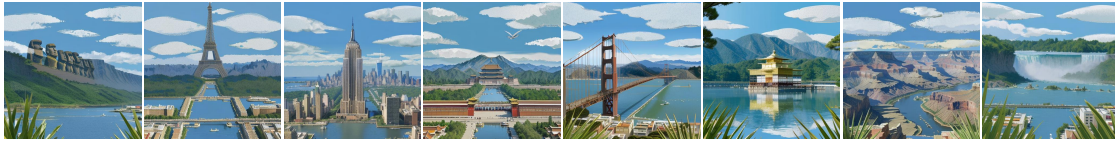


Griffith Observatory, Los Angeles    La Sagrada Familia, Barcelona    Matterhorn mountain, Swiss Alps    Mount Fuji    Neuschwanstein Castle, Bavaria    San Marco, Venice    Statue of Liberty    Louvre Museum, Paris

Figure 12. Additional results. Further demonstrations of style transfer efficacy.



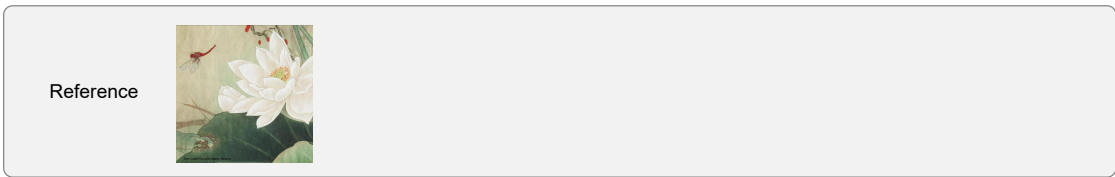
Great Pyramid of Giza    Great Wall of China    San Marco, Venice    Bran Castle (Dracula's Castle), Romania    Burj Khalifa, Dubai    Cathedral of Santa Maria del Fiore    Colosseum    Stonehenge



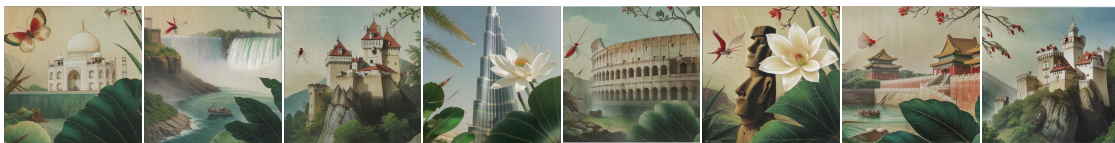
Easter Island    Eiffel Tower    Empire State Building, New York    Forbidden City, Beijing    Golden Gate Bridge, San Francisco    Golden Temple, Kyoto    Grand Canyon    Niagara Falls



La Sagrada Familia, Barcelona    Louvre Museum, Paris    Machu Picchu, Peru    Statue of Liberty    Mount Fuji    Neuschwanstein Castle, Bavaria    Sydney Opera    Sydney Opera



Cathedral of Santa Maria del Fiore    San Marco, Venice    Statue of Liberty    Stonehenge    Sydney Opera    Neuschwanstein Castle, Bavaria    Eiffel Tower    Great Pyramid of Giza



Taj Mahal    Niagara Falls    Bran Castle (Dracula's Castle), Romania    Burj Khalifa, Dubai    Colosseum    Easter Island    Forbidden City, Beijing    Bran Castle (Dracula's Castle), Romania



Golden Gate Bridge, San Francisco    Golden Temple, Kyoto    Grand Canyon    Great Wall of China    Griffith Observatory, Los Angeles    La Sagrada Familia, Barcelona    Louvre Museum, Paris    Machu Picchu, Peru

Figure 13. Additional results. Further demonstrations of style transfer efficacy.

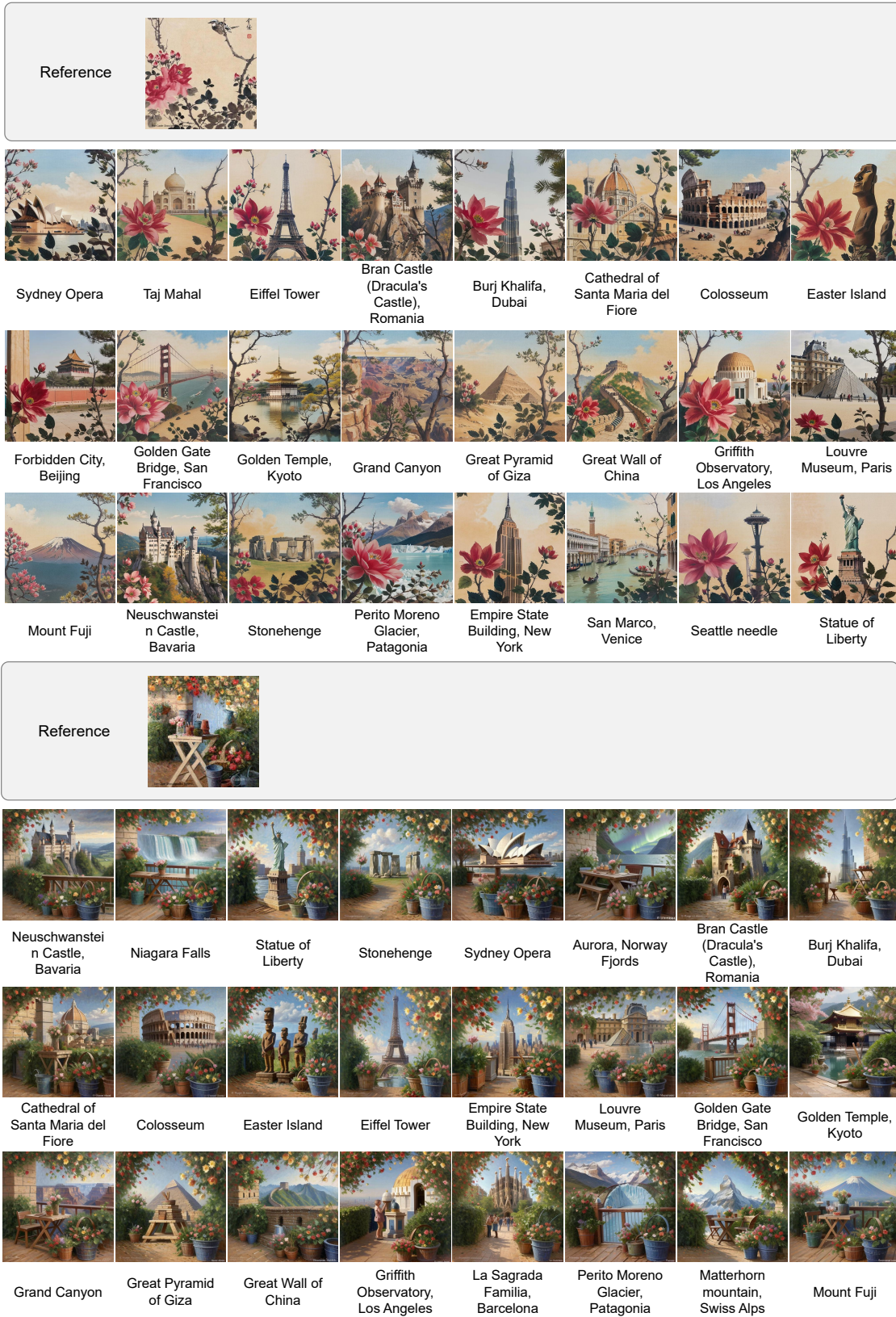


Figure 14. Additional results. Further demonstrations of style transfer efficacy.

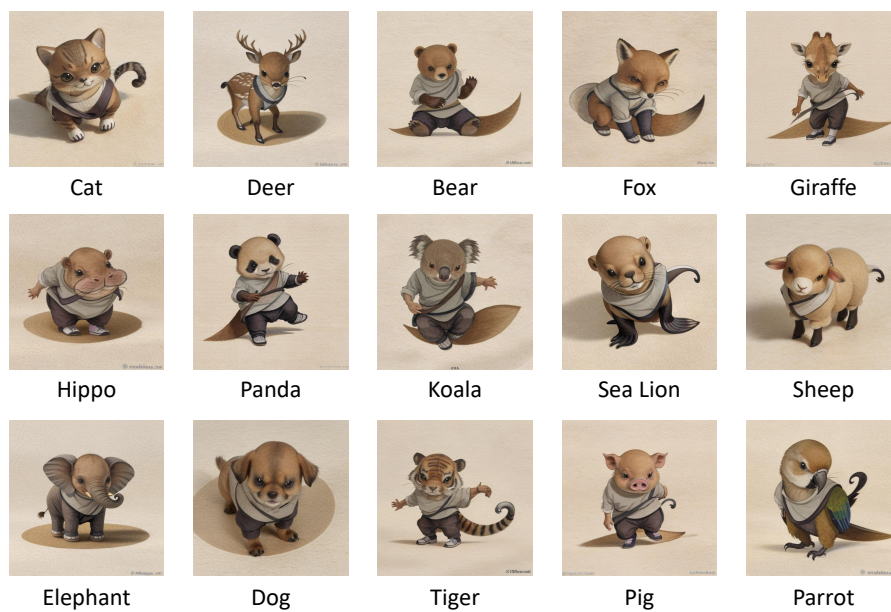
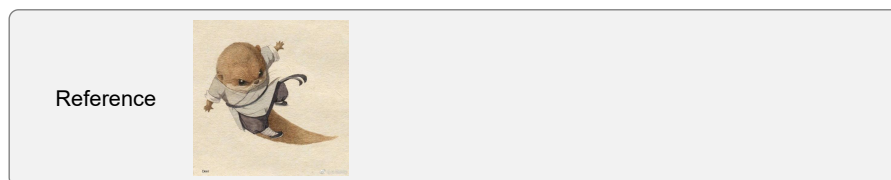
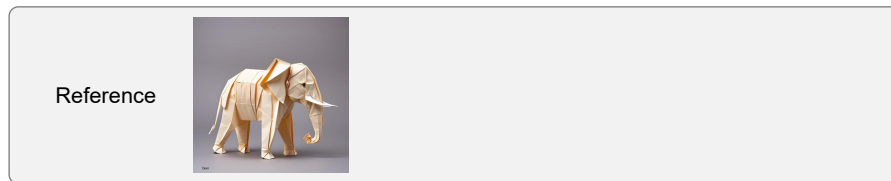


Figure 15. Additional results. Further demonstrations of style transfer efficacy.

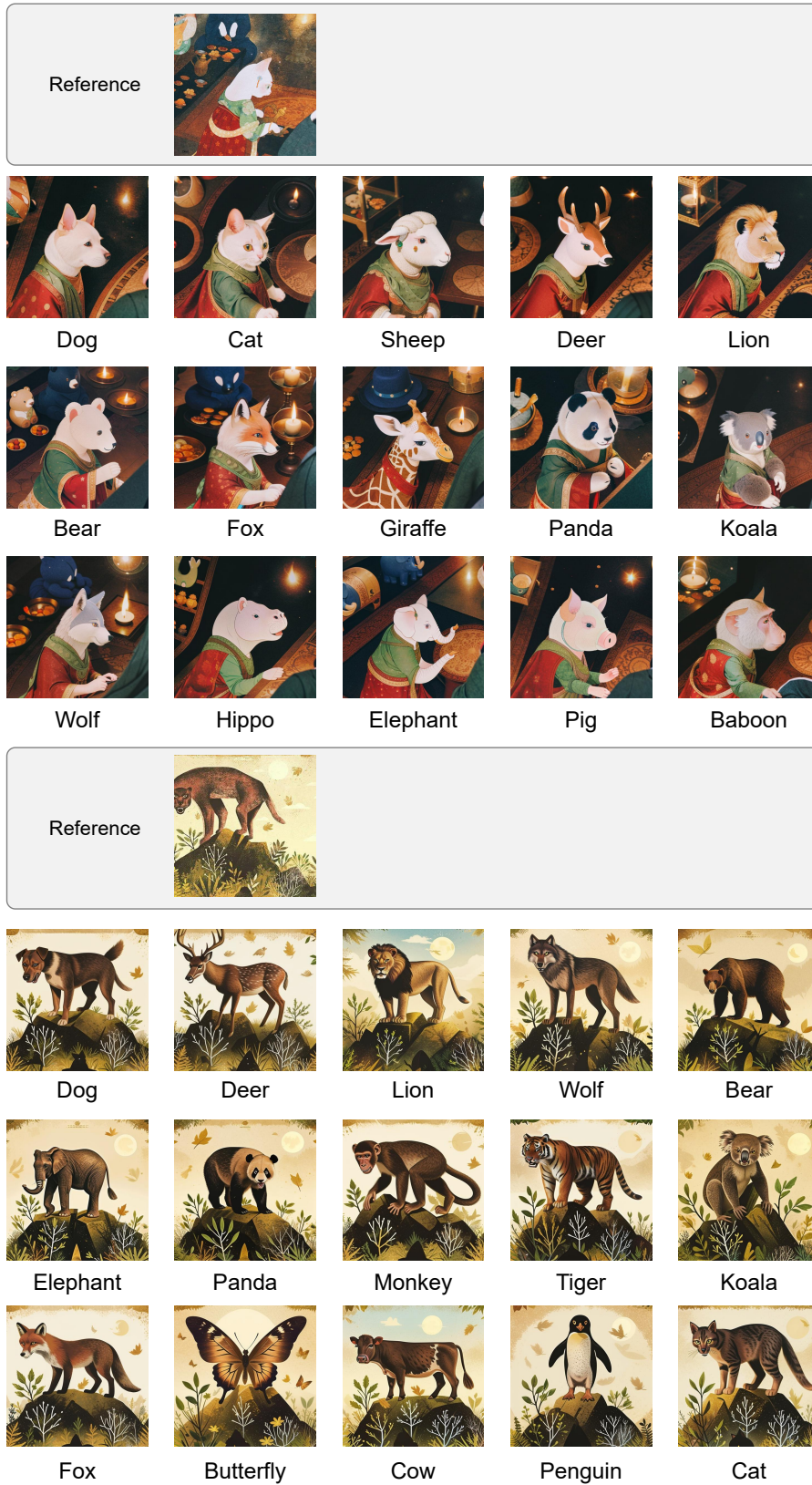


Figure 16. Additional results. Further demonstrations of style transfer efficacy.

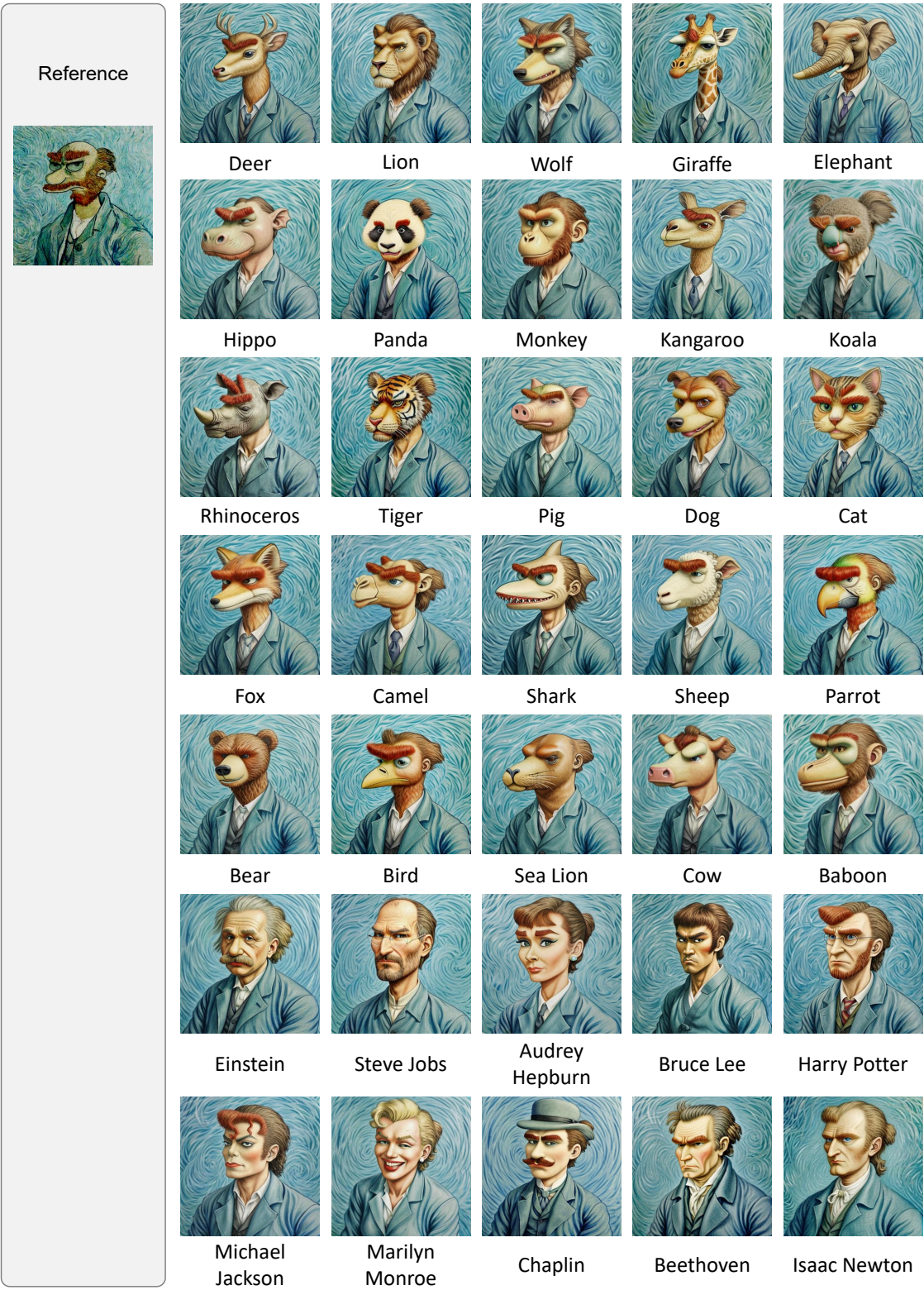


Figure 17. Additional results. Further demonstrations of style transfer efficacy.